New Phytologist

Do quantitative vessel and pit characters account for ion-mediated changes in the hydraulic conductance of angiosperm xylem?

Steven Jansen[1,2], Emmanuelle Gortan[3], Frederic Lens[4], Maria Assunta Lo Gullo[5], Sebastiano Salleo[3], Alexander Scholz[1], Anke Stein[1], Patrizia Trifilò[5] and Andrea Nardini[3]

[1]Institute for Systematic Botany and Ecology, Ulm University, Albert-Einstein-Allee 11, D–89081, Ulm, Germany; [2]Jodrell Laboratory, Royal Botanic Gardens, Kew, Richmond, Surrey, TW9 3DS, UK; [3]Dipartimento di Scienze della Vita, Università di Trieste, Via L. Giorgieri 10, I–34127 Trieste, Italia; [4]Laboratory of Plant Systematics, Institute of Botany and Microbiology, Kasteelpark Arenberg 31 Box 2437, K.U. Leuven, BE–3001 Leuven, Belgium; [5]Dipartimento di Scienze della Vita, Università di Messina, Salita Sperone 31, I–98166 Messina S. Agata, Italia

Author for correspondence:
Steven Jansen
Tel: +49 (0)731 5023302
Email: steven.jansen@uni-ulm.de

Received: *20 May 2010*
Accepted: *25 July 2010*

New Phytologist (2011) **189**: 218–228
doi: 10.1111/j.1469-8137.2010.03448.x

Key words: angiosperms, hydraulic conductivity, intervessel pit membrane, ionic effect, vessel grouping, wood anatomy.

Summary

- The hydraulic conductance of angiosperm xylem has been suggested to vary with changes in sap solute concentrations because of intervessel pit properties.
- The magnitude of the 'ionic effect' was linked with vessel and pit dimensions in 20 angiosperm species covering 13 families including six Lauraceae species.
- A positive correlation was found between ionic effect and vessel grouping parameters, especially the portion of vessel walls in contact with neighbouring vessels. Species with intervessel contact fraction (F_C) values < 0.1 showed an ionic effect between 2% and 17%, while species with F_C values > 0.1 exhibited a response between 10% and 32%. The ionic effect increased linearly with the mean fraction of the total vessel wall area occupied by intervessel pits as well as with the intervessel contact length. However, no significant correlation occurred between the ionic effect and total intervessel pit membrane area per vessel, vessel diameter, vessel length, vessel wall area, and intervessel pit membrane thickness.
- Quantitative vessel and pit characters are suggested to contribute to interspecific variation of the ionic effect, whereas chemical properties of intervessel pit membranes are likely to play an additional role.

Introduction

Long-distance water transport in vascular plants relies on the xylem tissue, which consists of a highly efficient conduit network connecting roots to the sites of water evaporation at leaf level (Sperry, 2003; Holbrook & Zwieniecki, 2005). The hydraulic conductance of xylem (K_h) strongly depends on the geometry of the conductive pipeline, in particular on their diameter and length according to the Hagen–Poiseuille law (Giordano *et al.*, 1978; Tyree & Zimmermann, 2002). Water transport in most woody angiosperms relies on a tortuous network of vessels, which do not pursue a strictly axial course, but make to some extent contact with other vessels (Braun, 1959, 1970). The vessel wall areas where neighbouring vessels are in contact with each other allow the passage of xylem sap from one vessel to another via intervessel pits, which is especially important given the limited axial length of a single vessel (Choat *et al.*, 2008; Neumann *et al.*, 2010). As water has to cross many thousands of intervessel pit membranes in order to move from the roots to the leaves, connectivity of the vessel network plays an important role in the magnitude of K_h in angiosperms (Choat *et al.*, 2006, 2008; Hacke *et al.*, 2006; Loepfe *et al.*, 2007).

Changes of K_h are a common consequence of xylem cavitation and embolism, a problem exacerbated by environmental stress such as drought, freezing and salinity (Cruiziat *et al.*, 2002; Tyree & Zimmermann, 2002). In addition, various studies suggest that K_h varies with changes in sap solute concentration in some woody dicot species, but also in few herbaceous angiosperms and ferns (Zimmermann, 1978; Van Ieperen *et al.*, 2000; Zwieniecki *et al.*, 2001; López-Portillo *et al.*, 2005; Nardini *et al.*, 2007a,b, 2010;

Trifilò *et al.*, 2008; Cochard *et al.*, 2010). The involvement of pit membranes in controlling K_h has been invoked as a possible explanation for this so-called ionic effect (Van Ieperen, 2007). The polyelectrolytic nature of pectins in intervessel pit membranes is thought to confer to these structures hydrogel properties (Ryden *et al.*, 2000; Ridley *et al.*, 2001; Willats *et al.*, 2001). Cations in the xylem sap can interfere with negative charges exposed in the pectin polysaccharides matrix, causing shrinking of pectins with consequent increase in the dimensions of pores in the pit membranes and final enhancement of K_h (Zwieniecki *et al.*, 2001). Although there is some experimental evidence for this hypothesis, there is no direct proof as it has not been possible to directly determine changes in pit membrane pores and pectin volume using microscopy. Hence, alternative explanations for ion-mediated changes of xylem hydraulic conductance should not be ruled out. As an example, electroviscous effects on liquid flow through pit membrane microchannels may result in similar effects on xylem water flow upon changes in sap ionic composition, without the need to invoke changes in pectin volume (Ren *et al.*, 2001). Although the physicochemical bases of the ionic effect clearly await further experiments to be fully understood, this phenomenon has been suggested to play a functional role *in planta* for the fine regulation of xylem water transport and alleviation of embolism-induced reduction of water supply to leaves (Zwieniecki *et al.*, 2004; Trifilò *et al.*, 2008; Nardini *et al.*, 2010).

The magnitude of the ionic effect is known to be variable across species and on a seasonal basis within a single species (Boyce *et al.*, 2004; Gascó *et al.*, 2006, 2007). Upon perfusion of stems with a solution of 20 mM KCl, K_h has been reported to be enhanced, compared with pure water, by up to 30% in some angiosperm species, while other species show hardly any response to changes in sap ionic content (Boyce *et al.*, 2004; López-Portillo *et al.*, 2005). However, measurements of the ionic effect, as conducted in some previous studies should be interpreted carefully as the use of deionized water as reference solution has been demonstrated to result in serious overestimations of the ion-mediated flow changes occurring *in planta* (Van Ieperen & Van Gelder, 2006; Nardini *et al.*, 2007b). Variation in the ionic effect has been suggested to reflect phylogenetic differences in the distribution of lignins and pectins in cell walls across vascular plants (Boyce *et al.*, 2004). In addition to the lignification hypothesis (Boyce *et al.*, 2004), recent evidence illustrates that the nature of pit membrane pectins is at least partly associated with the magnitude of the ionic effect in Lauraceae (E. Gortan *et al.*, unpublished).

Because the structural and functional basis of the variable response of the ionic effect in angiosperms is still unknown, this paper is aimed at elucidating the relationship between interspecific variation of the ionic effect and vessel characteristics. More specifically, the main question is whether the magnitude of the ionic effect is associated with quantitative vessel features such as vessel length, vessel diameter, vessel grouping and intervessel pitting. If intervessel pit membranes are indeed involved in the ionic effect, it is hypothesized that the ionic effect will be more pronounced in xylem with short, highly connected vessels than in xylem with long, solitary vessels. Although many studies have illustrated the large variation in vessel grouping both across woody angiosperms and within particular families (Braun, 1959, 1970; Zimmermann & Tomlinson, 1966, 1967; Carlquist, 1966, 1984, 1987, 2009; Rosell *et al.*, 2007; Lens *et al.*, 2009), functional consequences of the three-dimensional vessel network with respect to hydraulic traits remain poorly explored (Wheeler *et al.*, 2005; Hacke *et al.*, 2006; Loepfe *et al.*, 2007). As far as we know, no previous studies have investigated variation of the ionic effect in relation to quantitative vessel and pit dimensions in wood.

Materials and Methods

Plant material

Stem branches 1- to 4-yr-old were collected from plants growing at the botanical garden of the University of Trieste (Italy), the campus of the Faculty of Sciences at the University of Messina (Sicily), and from the living collections of the Royal Botanic Gardens, Kew (UK). Anatomical and hydraulic measurements were conducted on several branches from only one tree or shrub per species for a total number of 20 species (Table 1). As intraspecific and even intrasample variation in pit morphological features can be considerable (Domec *et al.*, 2008; Jansen *et al.*, 2004, 2009; Schoonmaker *et al.*, 2010), we were unable to assess the influence of intraspecific variation or phenotypic plasticity in this study. Although this limitation may compromise the assumption that trait values were representative for some species, the assumption that intraspecific variation was smaller than interspecific variation with respect to hydraulic traits provided a valid approach (Matzner *et al.*, 2001; Maherali *et al.*, 2006; Magnani, 2009; Martínez-Vilalta *et al.*, 2009). The species selected covered 13 families, including six Lauraceae species, and represented both evergreen and deciduous plants. Species selection depended on availability of fresh plant material at the University of Trieste and Messina. In addition to *Persea americana* Mill. from Messina, we sampled five Lauraceae species from Kew in order to test for variation of the ionic effect within closely related species. Twigs that were *c.* 50 cm long, 5–10 mm thick, and sun-exposed at the southwest to southeast part of the crown, were cut off in the field and immediately transported to the laboratory for hydraulic measurements. Fresh samples were put in a zip-seal bag with wet paper towels and shipped to the Royal Botanic Gardens, Kew (UK) for anatomical preparation.

Table 1 List of species studied with reference to their taxonomic family, sampling location, species acronym (as used in the figures) and magnitude of the ionic effect (i.e. the increase in xylem hydraulic conductance after adding 25 mM KCl to a reference solution) based on three to five branches from one specimen per species

Species (Family); accession number	Species acronym	Sampling location	Ionic effect (%) ± SD
Quercus ilex L. (Fagaceae)	Qi	Trieste	1.9 ± 1.1
Platanus orientalis L. (Platanaceae)	Po	Messina	4.7 ± 4.1
Litsea sericea (Wallich ex Nees) Hooker fil. (Lauraceae); 1994–3890	Ls	Kew	6.7 ± 2.8
Robinia pseudoacacia L. (Fabaceae)	Rp	Trieste	7.1 ± 1.7
Phillyrea latifolia L. (Oleaceae)	Phl	Trieste	8.4 ± 3.1
Lindera megaphylla Hemsl. (Lauraceae); 1913–52807	Lm	Kew	9.7 ± 3.4
Populus tremula L. (Salicaceae)	Pt	Trieste	11.1 ± 1.9
Arbutus unedo L. (Ericaceae)	Au	Messina	11.7 ± 3.7
Viburnum tinus L. (Adoxaceae)	Vt	Trieste	15.5 ± 2.1
Ceratonia siliqua L. (Fabaceae)	Cs	Messina	16.9 ± 6.6
Prunus laurocerasus L. (Rosaceae)	Prl	Trieste	17.1 ± 6.3
Neolitsea sericea (Blume) Koidz. (Lauraceae); 1989–3735	Ns	Kew	18.0 ± 0.3
Phytolacca dioica L. (Phytolaccaceae)	Pd	Messina	19.3 ± 8.7
Laurus nobilis L. (Lauraceae); 1972–12890	Ln	Kew	21.5 ± 8.2
Acer campestre L. (Sapindaceae)	Ac	Trieste	22.3 ± 8.1
Umbellularia californica (Hook. & Arn.) Nutt. (Lauraceae); 1988–2657	Uc	Kew	24.2 ± 1.1
Persea americana Mill. (Lauraceae)	Pa	Messina	27.3 ± 6.7
Citrus aurantium L. (Rutaceae)	Ca	Messina	28 ± 8
Olea europaea L. (Oleaceae)	Oe	Messina	31.5 ± 9.6
Nerium oleander L. (Apocynaceae)	No	Messina	32.3 ± 6.1

Accession numbers are given for Kew samples; species order is according to the magnitude of the ionic effect.

Hydraulic measurements

All hydraulic measurements were performed using well-established techniques (Gascó *et al.*, 2006, 2007) on three to five branches per species. Owing to variation of the ionic effect on a seasonal basis (Gascó *et al.*, 2007), samples were collected between April and July 2008 and 2009, that is, during spring and early summer. Stems were trimmed under water and immediately connected to a 'Xyl'em apparatus' (Bronkhorst, Montigny-les-Cormeilles, France). Because the magnitude of the ionic effect is influenced by the percentage of intact conduits in stem samples (Gascó *et al.*, 2006), vessel length distributions were assessed for each species (see the section entitled 'Vessel and pit dimensions'). The length of all stem samples used was such that at least 75% of all vessels remained intact. Hence, hydraulic measurements were based on samples from different species that have a similar proportion of intact vessels.

Eventual native embolism in the xylem was removed by perfusing the stem with a reference solution at a pressure of 0.2 MPa. We used two commercial mineral waters as reference fluid: Levissima (San Pellegrino SpA, Milan, Italy) for the Italian samples and Caledonian (Sainsbury's, London, UK) for the Kew samples (Table 1). The ion concentration for Levissima was 0.51 mM Ca^{2+}, 0.07 mM Mg^{2+}, 0.04 mM K^+, 0.08 mM Na^+, 0.03 mM NO_3^-, 0.96 mM HCO_3^-, 0.15 mM SO_4^{2-}, 0.01 mM F^-, and 0.03 mM Cl^- (data from the supplier). The Caledonian water included 0.67 mM Ca^{2+}, 0.27 mM Mg^{2+}, 0.02 mM K^+, 0.28 mM Na^+, 0.04 mM NO_3^-, 1.68 mM HCO_3^-, 0.11 mM SO_4^{2-}, 0.005 mM F^-, and 0.18 mM Cl^- (data from the supplier). The pH of both mineral waters was 7.4 (data from the supplier) and the overall osmolality was *c.* 5 mOsm kg^{-1}, which is similar to what is commonly found in native xylem sap. By using these reference fluids, we avoided spurious hydraulic effects caused by the use of deionized water and conducted hydraulic measurements using a solution that was considered to simulate the xylem sap ionic concentration better than fluids containing only few cations (Van Ieperen & Van Gelder, 2006; Nardini *et al.*, 2007b). The K_h was initially measured during perfusion of stems at a pressure of 8 kPa. Then, the fluid was enriched with 25 mM KCl and the eventual increase of K_h was measured when the flow became stable, which usually took between 30 min and 1 h. KCl is a suitable solute because K^+ is the most abundant cation in the xylem sap and represents *c.* 50% of total inorganic ion concentration (Siebrecht *et al.*, 2003). All perfusion solutions were filtered to 0.1 μm to prevent conduit clogging by suspended particles. Hydraulic measurements were conducted at a temperature of 20 ± 2°C.

Microscopy

Transverse wood sections *c.* 25 μm thick were prepared using a sliding microtome (Reichert, Vienna, Austria) and stained using a mixture of safranin and Alcian blue (35 : 65, v : v). The safranin solution was prepared as a 1% solution in 50% ethanol. The 1% Alcian blue stain was dissolved in deionized water. After staining, sections were washed in water, dehydrated in an ethanol series, treated with the clearing agent Histoclear (Fisher Scientific Ltd, Loughborough, UK) and embedded in Euparal (Agar Scientific Ltd, Essex, UK). Photographs of the two most recent growth rings were taken with an Axiocam HRC (Zeiss) digital camera on a Leitz Diaplan microscope (Leica Microsystems, Wetzlar, Germany).

Two samples per species were prepared for scanning electron microscopy (SEM) following Jansen *et al.* (2008). Small stem segments were dehydrated in an ethanol series, air-dried, split in a tangential plane, fixed to aluminium stubs with electron conductive carbon cement (Neubauer Chemikalien, Münster, Germany) and coated with platinum using an Emitech K550 sputter coater (Emitech Ltd, Ashford, UK). Samples were observed with a Hitachi S-4700 field-emission scanning electron microscope (Hitachi High Technologies Corporation, Tokyo, Japan) at an accelerating voltage of 2 kV.

A subset of 10 species that cover a wide range of the magnitude of the ionic effect was selected for transmission electron microscopy (TEM). Preparation of TEM samples was according to Jansen *et al.* (2009). Fresh wood from the last growth ring was fixed overnight in Karnovsky's fixative at room temperature. After washing in a 0.05 M phosphate buffer, the specimens were postfixed in 1% buffered OsO_4 for 4 h at room temperature, washed again, and dehydrated through a graded ethanol series. The ethanol was gradually replaced with LR White resin (London Resin Company, Reading, UK) over several days, and the resin was polymerized in a Gallenkamp (Loughborough, UK) vacuum oven at 60°C and 1000 mbar for 24 h. Embedded samples were trimmed with a Leica EM specimen trimmer (Leica Microsystems) and sectioned with an ultramicrotome (Ultracut; Reichert-Jung, Vienna, Austria). Transverse sections between 60 and 90 nm were attached to Formvar (Agar Scientific, Stansted, UK) and 100 mesh copper grids. Counterstaining was conducted with uranyl acetate and lead citrate using a Leica EM Stain system (Leica Microsystems). Observations were carried out with a JEM-1210 transmission electron microscope (Jeol, Tokyo, Japan) at 80 kV accelerating voltage and digital images were taken using a MegaView III camera (Soft Imaging System, Münster, Germany).

Vessel and pit dimensions

A list of the quantitative vessel and pit characteristics measured including their definitions and units is given in Table 2.

Data on the vessel length distribution were obtained using injection with silicone (Sperry *et al.*, 2005). Briefly, stems were first flushed at a pressure of 0.2 MPa with a water

Table 2 Wood anatomical characters measured for quantifying vessel and pit characters with their definitions and units

Acronym	Definition	Microscope	Units
Characters directly measured			
A_{PIT}	Intervessel pit membrane area	SEM	μm^2
D_{RL}	Vessel diameter corresponding to mean vessel lumen resistivity based on Hagen–Poiseuille equation	LM	μm
D_{PA}	Diameter of outer pit aperture as measured at the widest part of the opening	SEM	μm
D_{PM}	Horizontal pit membrane diameter at its widest point	SEM	μm
F_C	Intervessel contact fraction = portion of vessel wall in contact with other vessels based on transverse sections; = intervessel wall perimeter over total vessel wall perimeter	LM	No units
F_L	Intervessel contact length fraction = $L_C/L = 1 - V_S$	LM	No units
F_{PF}	Intervessel pit-field fraction = ratio of intervessel wall area occupied by pits to total intervessel wall area	SEM	No units
F_{VM}	Vessel multiple fraction = ratio of grouped vessels to total number of vessels	LM	No units
L	Average vessel length; since vessel length distributions are short-skewed, log-transformed mean lengths are used	LM	cm
T_{PM}	Intervessel pit membrane thickness	TEM	nm
T_V	Intervessel wall thickness measured as the double wall in the middle of adjacent vessels	LM	μm
V_G	Vessel grouping index = ratio of total number of vessels to total number of vessel groupings (including solitary and grouped vessels)	LM	No units
V_S	Solitary vessel index = ratio of total number of solitary vessels to total vessel groupings (including solitary and grouped vessels); = proportion of vessel length not in contact with adjacent vessels	LM	No units
Characters derived			
A_P	Total intervessel pit membrane area per vessel = $A_V \times F_P$		mm^2
A_V	Vessel wall area = $\pi D_{RL} L$		mm^2
F_P	Intervessel pit fraction = mean fraction of the total vessel wall area occupied by intervessel pits; = $F_C \times F_{PF}$		No units
L_C	Intervessel contact length = average contact length between adjacent vessels = $L \times F_L$		cm

LM, light microscopy; SEM, scanning electron microscopy; TEM, transmission electron microscopy.

reference solution (see the previous section entitled 'Hydraulic measurements') to remove emboli and then injected with a silicone mixture at P = 0.5 MPa for 3 h. Rhodorsil RTV-141 (Rhodia, Cranbury, NJ, USA) was used as two-component silicone elastomer for all samples from Italy, and QSil218 (ACC Silicones Ltd, Bridgewater, UK) was used for plant material from the UK. Both silicone elastomers show similar properties with respect to curing conditions, pot life and viscosity. Application of both silicone elastomers to stems from the same species showed no significant difference in vessel length distribution, indicating that these silicones do not pass pit membranes. In order to better visualize the silicone, 1 g of a blue pigment (Pentasol; Prochima, Pesaro, Italy) was added to the Rhodorsil elastomer and 1 drop of 1% (w : w) Uvitex optical brightener (Ciba UK Plc., Bradford, West Yorkshire, UK) dissolved in chloroform per gram of QSil218 silicone. Silicone hardening was complete after 12 h of air-drying. Samples were then cut into 1.5- to 3-cm long pieces. Transverse sections (*c.* 20–50 μm thick) were cut by hand with razor blades and observed immediately under a light microscope for silicone mixed with Pentasol and a fluorescent light microscope for Uvitex. For each section, the number of vessels filled with silicone was counted in order to obtain the vessel length distribution and average vessel length (L), which was calculated using the equations reported by Sperry *et al.* (2005) based on three to five stem branches per species. Log-transformed mean lengths are reported because of the generally short-skewed length distributions.

The vessel diameter (D_{RL}) was calculated as the diameter corresponding to mean lumen resistivity (R_L) using the Hagen–Poiseuille equation. Mean D_{RL} values were based on a minimum of 300 vessels.

Various vessel grouping indices were calculated based on a total number of > 500 vessels per species using LM images. The vessel grouping index (V_G) was defined as suggested by Carlquist (1984, 2001). In addition, we calculated the solitary vessel index (V_S) and vessel multiple fraction (F_{VM}) after quantifying the total number of vessels, solitary vessels, grouped vessels and vessel groupings in a minimum of five selected xylem areas varying from 0.3 to 2.5 mm^2 (Table 2). Both solitary vessels and grouped vessels (i.e. vessel multiples) were counted as a vessel group. Assuming that vessels end randomly, V_S values based on two-dimensional cross-sections are similar to the proportion of the vessel length that is not in contact with adjacent vessels. Hence, $1 - V_S$ gives the fraction of the vessel length that is in contact with another vessel. This value was defined as the vessel contact length fraction (F_L). Multiplication of F_L and L gives the average contact length between adjacent vessels (L_C).

Measurements to estimate the mean fraction of the total vessel wall area occupied by intervessel pits (i.e. the pit fraction, F_P) and the total intervessel pit membrane area per vessel (A_P) followed methods previously described in detail by Wheeler *et al.* (2005) and Hacke *et al.* (2006). Details are listed in Table 2. The intervessel contact fraction (F_C) was determined on a minimum of 500 vessels from five or more selected xylem areas between 0.3 mm^2 and 2.5 mm^2 based on three or more stems. The pit-field fraction (F_{PF}) was calculated on four or more SEM images of *c.* 0.1 mm^2 radial intervessel wall using two wood samples per species.

The total intervessel wall thickness (T_V) was measured as the double intervessel wall in the middle of two adjacent vessels that have a more or less similar diameter. The TEM images were used to measure the pit membrane thickness (T_{PM}). Average values for T_V and T_{PM} were based on a minimum of 25 measurements. Mean values for intervessel pit membrane area (A_{PIT}), pit membrane diameter (D_{PM}), and outer pit aperture diameter (D_A) were based on at least 50 measurements from SEM images of various intervessel walls.

Anatomical measurements were conducted using IMAGEJ (Rasband, 1997–2004).

Evaluating relationships

Statistical analyses were performed using the R statistical environment (R Development Core Team, 2008). For all tests, analyses were considered statistically significant if $P \leq 0.05$.

Results

The increase in hydraulic conductance after perfusing stems with a 25 mM KCl solution showed a large variation across the species studied, varying from 1.9% in *Quercus ilex* to > 30% in *Olea europaea* and *Nerium oleander* (Table 1). The average increase of the ionic effect across all species studied was 16.8% (± 9.04 SD), with 14 species showing mean values higher than 10%. The variation found within Lauraceae was substantial: the magnitude of the ionic effect measured was < 10% in *Litsea sericea* and *Lindera megaphylla*, but > 15% in four other Lauraceae species.

A summary of selected vessel and pit characteristics is given in Table 3. Several quantitative features were found to be correlated with the ionic effect (Table 4). The strongest correlation (r = 0.79, P < 0.0001) was found between the ionic effect and the vessel contact fraction (F_C). The latter varied from 0.01 in *Q. ilex* to 0.26 in *N. oleander* (Fig. 1a, Table 3), with an average F_C value of 0.11 (± 0.05 SD). While the pit-field fraction (F_{PF}), which was, on average, 0.54% (± 0.115 SD), showed no correlation with the ionic effect, the pit fraction (F_P) was positively correlated with the ionic effect (r = 0.73; P = 0.0003; Fig. 1b). Weaker correlations, although statistically significant (P < 0.02), were found between the ionic effect and vessel grouping features (V_G, V_S, F_{VM}): there was a general increase of the ionic effect in species with higher levels of

Table 3 Selected wood anatomical measurements related to vessel and pit characteristics for 20 angiosperms species

Species	D_{RL} (μm)	L (cm)	L_C (cm)	F_L (no units)	F_C (no units)	F_{PF} (no units)	V_G (no units)	T_{PM} (nm)	T_V (μm)
Qi	43.4 ± 12.5	11.4 ± 0.07	0.03 ± 0.04	0.003 ± 0.004	0.01 ± 0.008	0.53 ± 0.078	1.00 ± 0.004	689 ± 246	4.18 ± 1.54
Po	33.5 ± 7.3	5.29 ± 0.57	1.15 ± 0.32	0.218 ± 0.056	0.07 ± 0.015	0.39 ± 0.027	1.22 ± 0.06	129 ± 27	2.11 ± 0.21
Ls	31.2 ± 6.7	4.72 ± 0.49	1.66 ± 0.42	0.352 ± 0.081	0.10 ± 0.01	0.61 ± 0.071	1.41 ± 0.094	829 ± 133	5.33 ± 0.45
Rp	32.1 ± 10.9	10.9 ± 0.30	2.69 ± 0.95	0.247 ± 0.087	0.06 ± 0.015	0.52 ± 0.11	1.29 ± 0.095	119 ± 35	5.96 ± 1.94
Phl	21.1 ± 5.3	2.96 ± 0.36	0.62 ± 0.20	0.211 ± 0.064	0.07 ± 0.012	0.38 ± 0.027	1.25 ± 0.076	–	2.23 ± 0.86
Lm	34.6 ± 8.9	4.03 ± 0.48	1.63 ± 0.63	0.405 ± 0.149	0.11 ± 0.016	0.63 ± 0.057	1.59 ± 0.233	529 ± 94	6.46 ± 1.05
Pt	27.4 ± 7.5	7.88 ± 0.55	2.21 ± 0.46	0.281 ± 0.054	0.11 ± 0.015	0.60 ± 0.044	1.37 ± 0.065	–	5.07 ± 0.67
Au	12.9 ± 3.4	4.55 ± 0.62	0.86 ± 0.32	0.189 ± 0.066	0.06 ± 0.010	0.42 ± 0.044	1.20 ± 0.055	–	4.16 ± 0.98
Vt	20.7 ± 4.7	1.59 ± 0.04	0.28 ± 0.16	0.174 ± 0.1	0.08 ± 0.012	0.47 ± 0.092	1.16 ± 0.11	–	4.01 ± 1.25
Cs	27 ± 8.5	7.58 ± 0.59	3.83 ± 1.12	0.506 ± 0.143	0.17 ± 0.026	0.50 ± 0.07	1.79 ± 0.181	–	7.47 ± 1.44
Prl	21.1 ± 5.1	2.56 ± 0.36	0.65 ± 0.23	0.255 ± 0.081	0.09 ± 0.017	0.59 ± 0.064	1.32 ± 0.17	–	4.53 ± 1.15
Ns	24.2 ± 5.8	4.44 ± 0.49	2.06 ± 0.50	0.465 ± 0.101	0.12 ± 0.02	0.53 ± 0.019	1.55 ± 0.136	630 ± 189	4.39 ± 1.1
Pd	44 ± 11.6	5.39 ± 0.62	2.70 ± 0.75	0.500 ± 0.128	0.13 ± 0.025	0.71 ± 0.04	1.68 ± 0.204	–	7.95 ± 1.7
Ln	35.2 ± 9.2	10.1 ± 0.92	3.40 ± 0.83	0.335 ± 0.076	0.13 ± 0.016	0.53 ± 0.06	1.33 ± 0.116	743 ± 124	7.09 ± 1.67
Ac	27.7 ± 6.1	3.74 ± 0.32	0.93 ± 0.16	0.248 ± 0.038	0.14 ± 0.015	0.85 ± 0.014	1.36 ± 0.064	–	4.7 ± 0.77
Uc	41.8 ± 12.6	3.92 ± 0.48	1.63 ± 0.61	0.415 ± 0.148	0.12 ± 0.024	0.57 ± 0.018	1.55 ± 0.242	603 ± 152	7.71 ± 1.11
Pa	34.3 ± 9.9	7.88 ± 1.15	2.16 ± 0.57	0.275 ± 0.06	0.13 ± 0.025	0.58 ± 0.041	1.35 ± 0.069	–	6.84 ± 1.65
Ca	12.3 ± 2.8	4.26 ± 0.93	1.41 ± 0.51	0.330 ± 0.097	0.15 ± 0.022	0.61 ± 0.102	1.42 ± 0.134	–	5.18 ± 1.72
Oe	36.3 ± 8.9	4.73 ± 0.28	1.81 ± 0.43	0.383 ± 0.088	0.14 ± 0.018	0.47 ± 0.048	1.44 ± 0.141	669 ± 21.3	8.94 ± 1.62
No	20.2 ± 3.4	6.29 ± 0.58	4.38 ± 1.14	0.697 ± 0.170	0.26 ± 0.025	0.39 ± 0.07	2.67 ± 0.518	194 ± 6.19	7.99 ± 1.2

Acronyms for species and characters are according to Tables 1 and 2, respectively. Species order is based on the magnitude of the ionic effect (Table 1). Values given represent mean values ± SD; T_{PM} data only available for 10 species studied by transmission electron microscopy; –, no data available.

Table 4 Pearson correlation analysis between the ionic effect and various anatomical characters based on average values from 20 angiosperm species

Anatomical character	*r*	*P*
A_P, total intervessel pit membrane area per vessel	0.42	0.0666
A_{PIT}, intervessel pit membrane area	−0.15	0.5151
A_V, vessel wall area	−0.25	0.2838
D_{PA}, diameter of pit aperture	−0.12	0.6210
D_{PM}, diameter of pit membrane	−0.05	0.8467
D_{RL}, vessel diameter	−0.13	0.5868
F_C, intervessel contact fraction	**0.79**	**< 0.0001**
F_L, intervessel contact length fraction	**0.59**	**0.0067**
F_P, intervessel pit fraction	**0.73**	**0.0003**
F_{PF}, intervessel pit-field fraction	0.13	0.5850
F_{VM}, vessel multiple fraction	**0.62**	**0.0037**
L, vessel length	−0.19	0.4177
L_C, intervessel contact length	0.43	0.0588
T_{PM}, intervessel pit membrane thickness	0.07	0.8557
T_V, intervessel wall thickness	**0.65**	**0.0018**
V_G, vessel grouping index	**0.55**	**0.0127**
V_S, solitary vessel index	**−0.59**	**0.0067**

Significant correlations ($P < 0.05$) are shown in bold type. Full definitions of anatomical characters are given in Table 2.

grouped vessels (i.e. high values of V_G, F_{VM}) compared with species that had a high proportion of solitary vessels (Fig. 2a,b). The solitary vessel index (V_S) decreased with increasing values of ionic effect ($r = -0.59$, $P = 0.0067$; Fig. 2a). Minor differences were found between the vessel grouping parameters V_G, V_S and F_{VM}, with F_{VM} and V_S showing a higher correlation with the ionic effect than V_G (Table 4). As the intervessel contact length fraction (F_L) equals $1 - V_S$, a similar although positive correlation was found between F_L and ionic effect.

The ionic effect was not correlated with the average vessel length (L) and only a weak correlation occurred between the ionic effect and the contact length between adjacent vessels (L_C; $r = 0.43$, $P = 0.0588$). Except for the correlation between L and A_P ($r = 0.47$, $P = 0.0372$) and a nonsignificant correlation between L and D_{RL} ($r = 0.43$, $P = 0.0568$), L was not correlated with other pit and vessel grouping characters.

No correlation was found between the ionic effect and vessel diameter (D_{RL}) and vessel area (A_V). Moreover, our data revealed only a weak and nonsignificant correlation between the ionic effect and the total area of intervessel pit membranes per vessel (A_P; $r = 0.43$, $P = 0.0666$, Fig. 3). The correlation between the ionic effect with F_C and F_P remained strong ($P < 0.001$), while no significant correlation was found with A_P when excluding the six Lauraceae species from our dataset or when analysing the Lauraceae separately.

At the pit level, quantitative pit characteristics (A_{PIT}, D_{PA}, D_{PM}) showed no correlation with the ionic effect

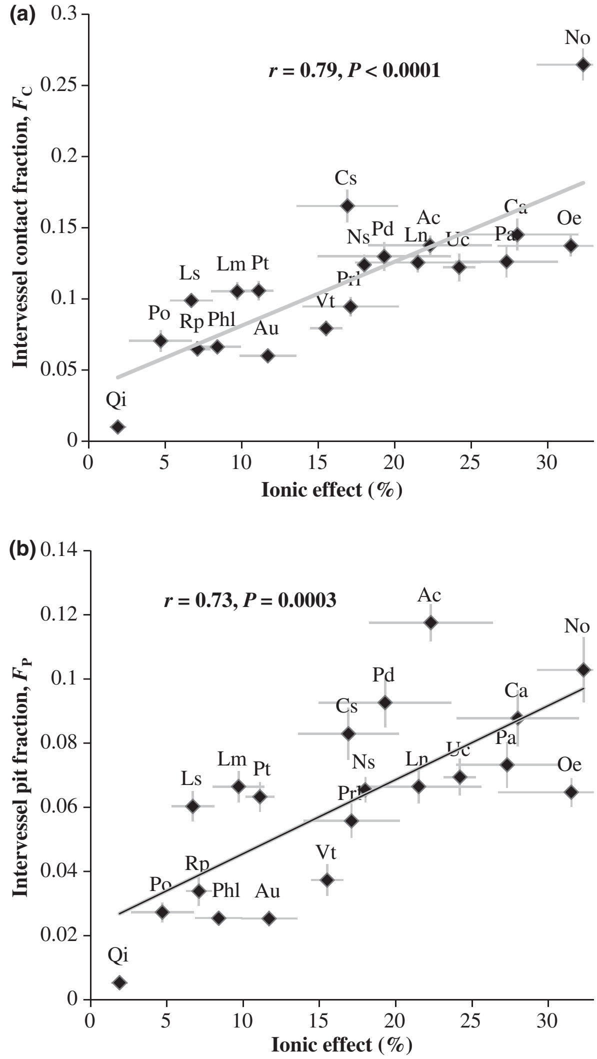

Fig. 1 (a) Intervessel contact fraction (F_C) and (b) intervessel pit fraction (F_P) plotted as a function of ionic effect (%) across 20 angiosperm species. Data represent average values per species ± SD. Species acronyms and definitions are according to Table 1, 2.

(Table 4; average values per species not shown). While the pit membrane thickness (T_{PM}) was not associated with variation of the ionic effect, there was a significant and positive correlation between intervessel wall thickness (T_V) and ionic effect ($r = 0.65$, $P = 0.0018$). Intervessel pit membranes were, on average, 513 nm (± 265 nm SD). Thin pit membranes (< 200 nm) occurred in *Platanus orientalis*, *Robinia pseudoacacia*, and *N. oleander*, while much thicker ones (> 700 nm) were observed in *Laurus nobilis* and *L. sericea*.

Discussion

Our dataset illustrates significant correlations between the ionic effect and quantitative vessel characteristics, such as

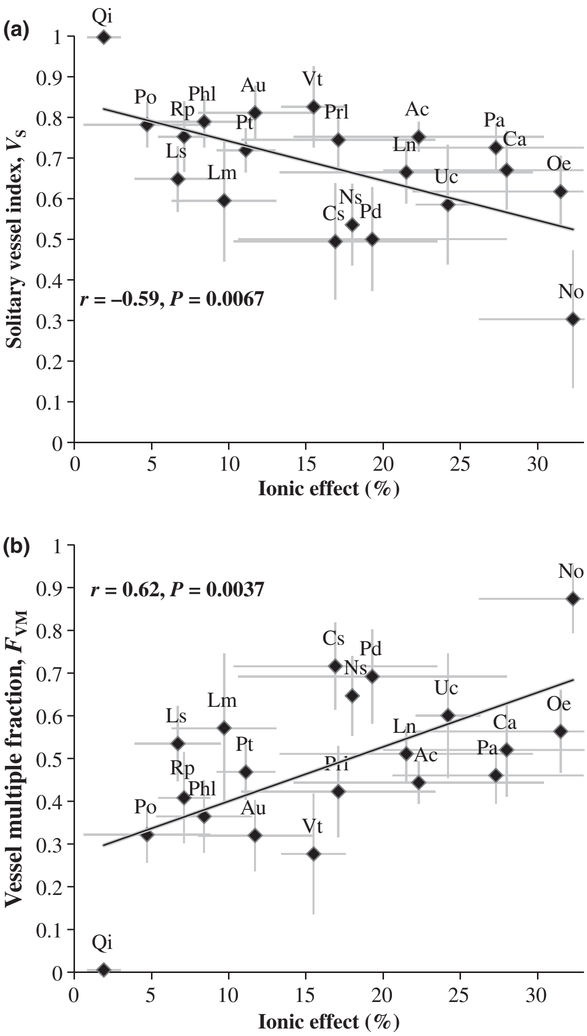

Fig. 2 (a) Solitary vessel index (V_S) and (b) vessel multiple fraction (F_{VM}) vs ionic effect (%) across 20 angiosperm species. Data represent average values per species ± SD. Species acronyms and definitions are according to Table 1, 2.

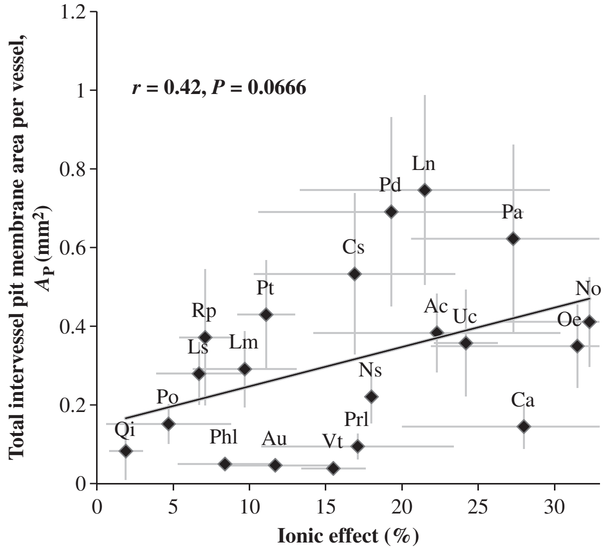

Fig. 3 Total intervessel pit membrane area per vessel (A_P) vs ionic effect across 20 angiosperm species. Data represent average values per species ± SD. Species acronyms and definitions are according to Table 1, 2.

vessel grouping characters (F_C, F_{VM}, V_G and V_S) and the intervessel pit fraction (F_P). F_C quantifies the actual overlap between neighbouring vessels more precisely than V_G, V_S and F_{VM}, because F_C takes into account the actual amount of intervessel overlap, while V_G, V_S and F_{VM} are only based on absolute numbers of solitary vessels, vessel multiples, and vessel groupings. A_P values, which are an estimate of the absolute quantity of intervessel pitting within a vessel of average vessel length and diameter, show only a weak correlation with the ionic effect. These findings seem to imply that the relative estimate of intervessel contact within the hydraulic vessel network plays a role in the magnitude of the ionic effect. In general, intervessel grouping received rather limited attention in earlier studies on hydraulic traits (Huggett & Tomlinson, 2010) and can traditionally be considered as sufficiently high throughout plants, even in species with a relatively large amount of solitary vessels. Intervessel overlap and pitting was therefore not interpreted as an essential parameter that determines hydraulic constraints. So far, most attention to explain variation in K_h has been paid to vessel diameter, vessel length and vessel density (Tyree & Zimmermann, 2002; Ewers *et al.*, 2007; Sperry *et al.*, 2008; McCulloh *et al.*, 2010). It is clear that progress in understanding water transport in plants may benefit from linking hydraulic parameters with quantitative interconduit features (Choat *et al.*, 2008; Hacke & Jansen, 2009).

The average F_C value obtained for *N. oleander* (0.26 ± 0.02), which shows up to 10 vessels arranged in radial multiples, is much higher than the F_C values measured for all other species studied. Similarly high F_C values as in *N. oleander* have been reported in *Acer grandidentatum* (Hacke *et al.*, 2006) and various *Acer* species (F. Lens *et al.*, unpublished). It would be interesting to find out if the ionic effect of 22.3% (± 8.1% SD) as reported here for *Acer campestre* corresponds to comparable levels of ionic effect in other species of *Acer*. A high F_C value (0.35 ± 0.013 SE) has also been recorded in the fern *Pteridium aquilinum* (Wheeler *et al.*, 2005). Very high levels of ionic effect have been measured in ferns, with an average increase of K_h *c.* 68% (± 21% SD) based on five fern species, including one species of *Pteridium* (Boyce *et al.*, 2004). Although the ionic effect measurements reported by Boyce *et al.* (2004) should be interpreted with caution because of the use of deionized water as reference fluid (Van Ieperen & Van Gelder, 2006; Nardini *et al.*, 2007b), the high F_C value in combination with the high response to the ionic effect in five ferns (Wheeler *et al.*, 2005; Boyce *et al.*, 2004) suggest that *P. aquilinum* has a potentially high ionic effect. We note that the average ionic effect for 30 angiosperm species was 32% (± 16% SD) as reported by Boyce *et al.* (2004), which is considerably higher than the average of 16.8% (± 9% SD) based on the 20 species selected for this study. Most likely, the difference between both studies can be explained by the ionic concentration of the reference solution.

Besides *Nerium oleander*, vessel grouping indices (V_G) were relatively low (< 2) and showed rather limited variation across our sampling. As much higher V_G values (i.e. > 20) have been reported in several climbing Apocynaceae (Lens *et al.*, 2009) and in various angiosperm families (Carlquist & Hoekman, 1985; Carlquist, 1984, 2009), it would be interesting to test whether or not species with higher V_G levels than reported in our sampling show an even more pronounced ionic effect than observed in *Nerium oleander* (32.3% ± 6.1 SD). Variation in V_G is usually thought to be genus- or species-specific, but depending on the taxonomic group is also found to characterize higher taxonomic levels (Carlquist, 1984; Lens *et al.*, 2008, 2009). As illustrated in Figs 1 and 2, there is considerable scattering among species when plotting the ionic effect vs vessel grouping characters, indicating that relatively large differences in ionic effect correspond to very little or no change in quantitative vessel grouping characters. Although the correlations shown in Figs 1 and 2 appear linear, increasing the percentage of loss of conductance (PLC) in stems of *Laurus nobilis* showed an exponential increase of ionic effect compared with fully hydrated stems after injection with 100 mM KCl (Gascó *et al.*, 2006). In particular, a PLC increase from 0% to 25% in stems of *L. nobilis*, which probably did not add very much to the amount of radial water transport, caused the ionic effect to double from 22% to *c.* 45% (Gascó *et al.*, 2006). Therefore, it is possible that minor changes in quantitative vessel characters (F_C, V_S, F_{VM}, V_G) have a considerable effect on the magnitude of the ionic effect across species (Figs 1 and 2).

Recent findings in seven species of *Acer* indicated that high values of V_G and F_C were associated with relatively short and narrow vessels (F. Lens *et al.*, unpublished). If short and narrow vessels (i.e. low L and D_{RL}) are indeed linked to high rates of V_G, F_{VM}, F_C, and thus F_P, but low values of V_S, it is possible that high values of F_C and F_P are compensated by low values of A_V (= $\pi D_{RL} L$), which would result in more or less steady values of A_P (= $A_V \times F_P$) across species with contrasting differences in hydraulic parameters such as ionic effect. Our present dataset, however, does not support this idea. Moreover, the strong correlations between A_P and resistance to drought-induced cavitation in angiosperm wood (Wheeler *et al.*, 2005; Hacke *et al.*, 2006) suggest that such an assumption cannot be generalized across a wide range of angiosperms. P_{50} values (i.e. the pressure that reduces hydraulic conductance by 50%) based on literature for a subset of 11 species studied in this paper did not show any correlation with the ionic effect.

Furthermore, imperforate tracheary elements should be considered when evaluating K_h and vessel grouping because of the strong correlation between V_G and the nature of imperforate tracheary elements (Carlquist, 1966, 1984, 1987, 2001, 2009; Rosell *et al.*, 2007). Careful observation of longitudinal sections showed that all species sampled in this study posses a fibrous ground tissue (i.e. fibre-tracheids and/or libriform fibres), except for *Viburnum tinus*, which has true tracheids. Moreover, vasicentric tracheids (i.e. tracheids surrounding vessel elements) occur in *Q. ilex*, *Phillyrea latifolia*, and *Arbutus unedo*. The distribution of true and vasicentric tracheids in our dataset is in line with low values of V_G and F_{VM}, but high values of V_S (Table 3; Carlquist, 1984). The magnitude of the ionic effect in the species with tracheids is below average, although no final conclusions can be made with respect to the impact of imperforate tracheary elements on the ionic effect because of limited sampling and minor variation in xylem ground tissue across the species studied.

In conclusion, this paper provides preliminary evidence that the quantity of vessel grouping and intervessel pitting contributes to interspecific variation of the ionic effect. As the correlation between the ionic effect and total intervessel pit membrane area per vessel (A_P; $r = 0.43$, $P = 0.0666$) was found to be only slightly weaker compared with a generally supported wood anatomical relationship such as vessel length (L) and vessel diameter (D_{RL}; $r = 0.43$, $P = 0.0568$; Zimmermann & Jeje, 1981; Hacke *et al.*, 2006; Huggett & Tomlinson, 2010), further work is needed to test the relationship between ionic effect and A_P. In addition to pit quantity, interspecific variation of the ionic effect is probably related to differences in pit membrane chemistry, in particular to the relative proportion of acidic vs methyl-esterified pit membrane pectins (Zwieniecki *et al.*, 2001; E. Gortan *et al.*, unpublished). Further chemical characterization of intervessel pit membranes would be most welcome to better understand ion-mediated changes of K_h. Future work is also needed to test whether the ionic effect is correlated with the relatively large variation in pit membrane area resistance (r_P) (Wheeler *et al.*, 2005; Choat *et al.*, 2006, 2008; Hacke *et al.*, 2006; Pittermann *et al.*, 2006).

Acknowledgements

Funding to SJ was provided by a grant from the 'Juniorprofessorenprogramm' of the Ministry of Science, Research, and the Arts (Baden-Wurttemberg, Germany). This study was partly funded by the University of Trieste (Finanziamento Ricerca di Ateneo 2008). Anonymous reviewers are acknowledged for useful comments and suggestions.

References

Boyce CK, Zwieniecki MA, Cody GD, Jacobsen C, Wirick S, Knoll AH, Holbrook NM. 2004. Evolution of xylem lignification and hydrogel transport regulation. *Proceedings of the National Academy of Sciences, USA* **101**: 17555–17558.

Braun HJ. 1959. Die Vernetzung der Gefäβe bei *Populus. Zeitschrift für Botanik* **47**: 421–435.

Braun HJ. 1970. *Funktionelle Histologie der sekundären Sprossachse I. Das Holz. Encyclopaedia of Plant Anatomy Band IX, Teil 1*. Berlin and Stuttgart, Germany: Gebrüder Borntraeger.

Carlquist S. 1966. Wood anatomy of Compositae: a summary, with comments on factors controlling wood anatomy. *Aliso* **6**: 25–44.

Carlquist S. 1984. Vessel grouping in dicotyledon wood: significance and relationship to imperforate tracheary elements. *Aliso* **10**: 505–525.

Carlquist S. 1987. Diagonal and tangential vessel aggregations in wood: function and relationship to vasicentric tracheids. *Aliso* **11**: 451–462.

Carlquist S. 2001. Comparative wood anatomy: systematic, ecological, and evolutionary aspects of dicotyledon wood. Berlin, Heidelberg, Germany: Springer-Verlag.

Carlquist S. 2009. Non-random vessel distribution in woods: patterns, modes, diversity, correlations. *Aliso* **27**: 39–58.

Carlquist S, Hoekman DA. 1985. Ecological wood anatomy of the woody southern Californian flora. *International Association of Wood Anatomists Bulletin* **6**: 319–347.

Choat B, Brodie TW, Cobb AR, Zwieniecki MA, Holbrook NM. 2006. Direct measurements of intervessel pit hydraulic resistance in two angiosperm tree species. *American Journal of Botany* **93**: 993–1000.

Choat B, Cobb A, Jansen S. 2008. Structure and function of bordered pits: new discoveries and impacts on whole plant hydraulic function. *New Phytologist* **177**: 608–626.

Cochard H, Herbette S, Hernández E, Hölttä T, Menuccini M. 2010. The effects of sap ionic composition on xylem vulnerability to cavitation. *Journal of Experimental Botany* **61**: 275–285.

Cruiziat P, Cochard H, Améglio T. 2002. Hydraulic architecture of trees: main concepts and results. *Annals of Forest Science* **59**: 723–752.

Domec J-C, Lachenbruch B, Meinzer FC, Woodruff DR, Warren JM, McCulloh KA. 2008. Maximum height in a conifer is associated with conflicting requirements for xylem design. *Proceedings of the National Academy of Sciences, USA* **105**: 12069–12074.

Ewers FW, Ewers JM, Jacobsen AL, López-Portillo J. 2007. Vessel redundancy: modelling safety in numbers. *International Association of Wood Anatomists Journal* **28**: 373–388.

Gascó A, Nardini A, Gortan E, Salleo S. 2006. Ion-mediated increase in the hydraulic conductivity of Laurel stems: role of pits and consequences for the impact of cavitation on water transport. *Plant, Cell & Environment* **29**: 1946–1955.

Gascó A, Salleo S, Gortan E, Nardini A. 2007. Seasonal changes in the ion-mediated increase of xylem hydraulic conductivity in stems of three evergreens: any functional role? *Physiologia Plantarum* **129**: 597–606.

Giordano R, Salleo A, Salleo S, Wanderlingh F. 1978. Flow in xylem vessels and Poiseuille's law. *Canadian Journal of Botany* **56**: 333–338.

Hacke UG, Jansen S. 2009. Embolism resistance of three boreal conifer species varies with pit structure. *New Phytologist* **182**: 675–686.

Hacke UG, Sperry JS, Wheeler JK, Castro L. 2006. Scaling of angiosperm xylem structure with safety and efficiency. *Tree Physiology* **26**: 619–701.

Holbrook NM, Zwieniecki MA. 2005. *Vascular transport in plants*. Burlington, VT, USA: Elsevier Academic Press.

Huggett B, Tomlinson PB. 2010. Aspects of vessel dimensions in the aerial roots of epiphytic Araceae. *International Journal of Plant Sciences* **171**: 362–369.

Jansen S, Choat B, Pletsers A. 2009. Morphological variation of intervessel pit membranes and implications to xylem function in angiosperms. *American Journal of Botany* **96**: 409–419.

Jansen S, Choat B, Vinckier S, Lens F, Schols P, Smets E. 2004. Intervascular pit membranes with a torus in the wood of *Ulmus* (Ulmaceae) and related genera. *New Phytologist* **163**: 51–59.

Jansen S, Pletsers A, Sano Y. 2008. The effect of preparation techniques on SEM-imaging of pit membranes. *International Association of Wood Anatomists Journal* **29**: 161–178.

Lens F, Endress ME, Baas P, Jansen S, Smets E. 2008. Wood anatomy of Rauvolfioideae (Apocynaceae): a search for meaningful non-DNA characters at the tribal level. *American Journal of Botany* **95**: 1199–1215.

Lens F, Endress ME, Baas P, Jansen S, Smets E. 2009. Vessel grouping patterns in subfamilies Apocynoideae and Periplocoideae confirm phylogenetic value of wood structure within Apocynaceae. *American Journal of Botany* **96**: 2168–2183.

Loepfe L, Martinez-Vilalta J, Pinola J, Mencuccini M. 2007. The relevance of xylem network structure for plant hydraulic efficiency and safety. *Journal of Theoretical Biology* **247**: 788–803.

López-Portillo J, Ewers FW, Angeles G. 2005. Sap salinity effects on xylem conductivity in two mangrove species. *Plant, Cell & Environment* **28**: 1285–1292.

Magnani F. 2009. Phenotypic variability: underlying mechanisms and limits do matter. *New Phytologist* **184**: 277–279.

Maherali H, Moura CF, Caldeira MC, Willson CJ, Jackson RB. 2006. Functional coordination between leaf gas exchange and vulnerability to xylem cavitation in temperate forest trees. *Plant, Cell & Environment* **29**: 571–583.

Martínez-Vilalta J, Cochard H, Mencuccini M, Sterck F, Herrero A, Korhonen JFJ, Llorens P, Nikinmaa E, Nolè A, Poyatos R *et al.* 2009. Hydraulic adjustment of Scots pine across Europe. *New Phytologist* **184**: 353–364.

Matzner SL, Rice KJ, Richards JH. 2001. Intraspecific variation in xylem cavitation in interior live oak (*Quercus wislizenii*). *Journal of Experimental Botany* **52**: 783–789.

McCulloh K, Sperry JS, Lachenbruch B, Meinzer FC, Reich PB, Voelker S. 2010. Moving water well: comparing hydraulic efficiency in twigs and trunks of coniferous, ring-porous, and diffuse-porous saplings from temperate and tropical forests. *New Phytologist* **186**: 439–450.

Nardini A, Gascó A, Cervone F, Salleo S. 2007a. Reduced content of homogalacturonan does not alter the ion-mediated increase in xylem hydraulic conductivity in tobacco. *Plant Physiology* **143**: 1975–1981.

Nardini A, Gascó A, Trifilò P, Lo Gullo MA, Salleo S. 2007b. Ion-mediated enhancement of xylem hydraulic conductivity is not always suppressed by the presence of Ca^{2+} in the sap. *Journal of Experimental Botany* **58**: 2609–2615.

Nardini A, Grego F, Trifilò P, Salleo S. 2010. Changes of xylem sap ionic content and stem hydraulics in response to irradiance in *Laurus nobilis* L. *Tree Physiology* **30**: 628–635.

Neumann PM, Weissman R, Stefano G, Mancuso S. 2010. Accumulation of xylem transported protein at pit membranes and associated reduction in hydraulic conductance. *Journal of Experimental Botany* **61**: 1711–1717.

Pittermann J, Sperry JS, Hacke UG, Wheeler JK, Sikkema EH. 2006. Inter-tracheid pitting and the hydraulic efficiency of conifer wood: the role of tracheid allometry and cavitation protection. *American Journal of Botany* **93**: 1265–1273.

R Development Core Team. 2008. *R: a language and environment for statistical computing*. Vienna, Austria: R Foundation for Statistical Computing.

Rasband WS. 1997–2004. *ImageJ*. Bethesda, MD, USA: National Institutes of Health [WWW document]. URL http://rsb.info.nih.gov/ij/ [accessed May 2009].

Ren L, Li D, Qu W. 2001. Electro-viscous effects on liquid flow in microchannels. *Journal of Colloid and Interface Science* **233**: 12–22.

Ridley BL, O'Neill MA, Mohnen D. 2001. Pectins: structure, biogenesis and oligogalacturonide-related signaling. *Phytochemistry* **57**: 929–967.

Rosell JA, Olson M, Aguirre-Hernández R, Carlquist S. 2007. Logistic regression in comparative wood anatomy: tracheid types, wood anatomical terminology, and new inferences from the Carlquist and Hoekman southern Californian data set. *Botanical Journal of the Linnean Society* **154**: 331–351.

Ryden P, MacDougall AJ, Tibbits CW, Ring SG. 2000. Hydration of pectic polysaccharides. *Biopolymers* **54**: 398–405.

Schoonmaker AL, Hacke UG, Landhäusser SM, Lieffers VJ, Tyree MT. 2010. Hydraulic acclimation to shading in boreal conifers of varying shade tolerance. *Plant, Cell & Environment* **33**: 382–393.

Siebrecht S, Herdel K, Schurr U, Tischner R. 2003. Nutrient translocation in the xylem of poplar: diurnal variations and spatial distribution along the shoot axis. *Planta* **217**: 783–793.

Sperry JS. 2003. Evolution of water transport and xylem structure. *International Journal of Plant Sciences* **164**: S115–S127.

Sperry JS, Hacke UG, Wheeler JK. 2005. Comparative analysis of end wall resistivity in xylem conduits. *Plant, Cell & Environment* **28**: 456–465.

Sperry JS, Meinzer FC, McCulloh K. 2008. Safety and efficiency conflicts in hydraulic architecture: scaling from tissues to trees. *Plant, Cell & Environment* **31**: 632–645.

Trifilò P, Lo Gullo MA, Salleo S, Callea K, Nardini A. 2008. Xylem embolism alleviated by ion-mediated increase in hydraulic conductivity of functional xylem: insights from field measurements. *Tree Physiology* **28**: 1505–1512.

Tyree MT, Zimmermann MH. 2002. Xylem structure and the ascent of sap. New York, NY, USA: Springer-Verlag.

Van Ieperen W. 2007. Ion-mediated changes of xylem hydraulic resistance *in planta*: fact or fiction? *Trends in Plant Sciences* **12**: 137–142.

Van Ieperen W, Van Gelder A. 2006. Ion-mediated flow changes suppressed by minimal calcium presence in xylem sap in *Chrysanthemum* and *Prunus laurocerasus*. *Journal of Experimental Botany* **57**: 2743–2750.

Van Ieperen W, Van Meeteren U, Van Gelder H. 2000. Fluid ionic composition influences hydraulic conductance of xylem conduits. *Journal of Experimental Botany* **51**: 769–776.

Wheeler JK, Sperry JS, Hacke UG, Hoang N. 2005. Inter-vessel pitting and cavitation in woody Rosaceae and other vesselled plants: a basis for a safety versus efficiency trade-off in xylem transport. *Plant, Cell & Environment* **28**: 800–812.

Willats WGT, McCartney L, Mackie W, Knox JP. 2001. Pectin: cell biology and prospects for functional analysis. *Plant Molecular Biology* **47**: 9–27.

Zimmermann MH. 1978. Hydraulic architecture of some diffuse-porous trees. *Canadian Journal of Botany* **56**: 2286–2295.

Zimmermann MH, Tomlinson PB. 1966. Analysis of complex vascular systems in plants: optical shuttle method. *Science* **152**: 72–73.

Zimmermann MH, Tomlinson PB. 1967. A method for the analysis of the course of vessels in wood. *International Association of Wood Anatomists Bulletin* **1**: 2–6.

Zimmermann MH, Jeje AA. 1981. Vessel-length distribution in stems of some American woody plants. *Canadian Journal of Botany* **59**: 1882–1892.

Zwieniecki MA, Melcher PJ, Feild TS, Holbrook NM. 2004. A potential role for xylem–phloem interactions in the hydraulic architecture of trees: effects of phloem girdling on xylem hydraulic conductance. *Tree Physiology* **24**: 911–917.

Zwieniecki MA, Melcher PJ, Holbrook NM. 2001. Hydrogel control of xylem hydraulic resistance in plants. *Science* **291**: 1059–1062.